Interpretation of chemical analyses and cement modules in flysch by (geo)statistical methods, example from the southern Croatia

Bralić, Nikolina; Malvić, Tomislav

Source / Izvornik: **Processes, 2022, 10**

Journal article, Published version
Rad u časopisu, Objavljena verzija rada (izdavačev PDF)

https://doi.org/10.3390/pr10050813

Permanent link / Trajna poveznica: https://urn.nsk.hr/urn:nbn:hr:169:529152

processes

MDPI

Article

Interpretation of Chemical Analyses and Cement Modules in Flysch by (Geo)Statistical Methods, Example from the Southern Croatia

Nikolina Bralić [1,*] and Tomislav Malvić [2]

[1] Cemex Hrvatska d.d., F. Tuđmana 45, HR-21212 Kaštel Sućurac, Croatia
[2] Faculty of Mining, Geology and Petroleum Engineering, University of Zagreb, Pierottijeva 6, HR-10000 Zagreb, Croatia; tomislav.malvic@rgn.hr
* Correspondence: nikolina.bralic@cemex.com

Abstract: This study included the testing of normal (Gaussian) distribution of input data and, consequently, spatially interpolating maps of chemical components and cement modules in the flysch. This deposit contains the raw material for cement production. The researched area is located in southern Croatia, near Split, as part of the exploited field "St. Juraj–St. Kajo". There are six lithological units: (1) alternation of marls and sandstones with inclusions of conglomerates, (2) marl, (3) calcsiltite, (4) calcarenite, (5) marl with nummulites, (6) debrites, and (7) clayey marl. All of them are deposited in the (a) northern and (b) southern beds. Only debrites are divided into the (a) western and (b) eastern layers. Those lithological units were divided technologically based on their cement modules (lime saturation factor (LSF), silicate module (SM), and aluminate module (AM)). The average thicknesses were analysed, followed by normality tests (Kolmogorov–Smirnov (K–S) and Shapiro–Wilk (S–W)) of the chemical analyses: CaO, SiO_2, Al_2O_3, Fe_2O_3, MgO, SO_3, Na_2O, K_2O, $CaCO_3$ (%) and three cement modules (LSF, SM, AM), available in the six lithological units. The normality tests were applied based on a number of input data. The further interpolation was performed using two methods, kriging and inverse distance weighting, mapping CaO (%), SiO_2 (%), and LSF (−) in three different lithological units. The interpolation methods were selected based on two criteria: (a) normality test pass or fail and (b) the amount of data. In total, 144 tests were calculated, including sets from 7 to 36 points. The results show the current situation in the quarry, after decades of production, making reliable the future predictions of cement raw material exploitation.

Keywords: raw material; cement; flysch; cement modules; Kolmogorov–Smirnov; Shapiro–Wilk; kriging; inverse distance weighting

Citation: Bralić, N.; Malvić, T. Interpretation of Chemical Analyses and Cement Modules in Flysch by (Geo)Statistical Methods, Example from the Southern Croatia. *Processes* **2022**, *10*, 813. https://doi.org/10.3390/pr10050813

Academic Editor: Yidong Cai

Received: 1 April 2022
Accepted: 18 April 2022
Published: 20 April 2022

1. Introduction

The goal of this research was to statistically test the normal distribution of data from the raw material for cement production. Analyses were carried out for chemical compounds and cement modules in each of the seven lithological units which exist in the exploited field "St. Juraj–St. Kajo". The field is located near Split (southern Croatia), at the foothills of Mt. Kozjak, with an altitude between 70 and 240 m. The average elongation is 6 km (NW–SE) with a width of 0.9 km, which is defined as an irregular polygon (Figure 1) with an area of 215.85 ha.

The first geological explorations in the area of the Split-Dalmatia county was carried out during the period of the Austro-Hungarian Empire [1–6]. More extensive researching was carried out after WWII, including more specific goals like detail mapping, depositional environments, engineering geology, and reserve calculation [7–18].

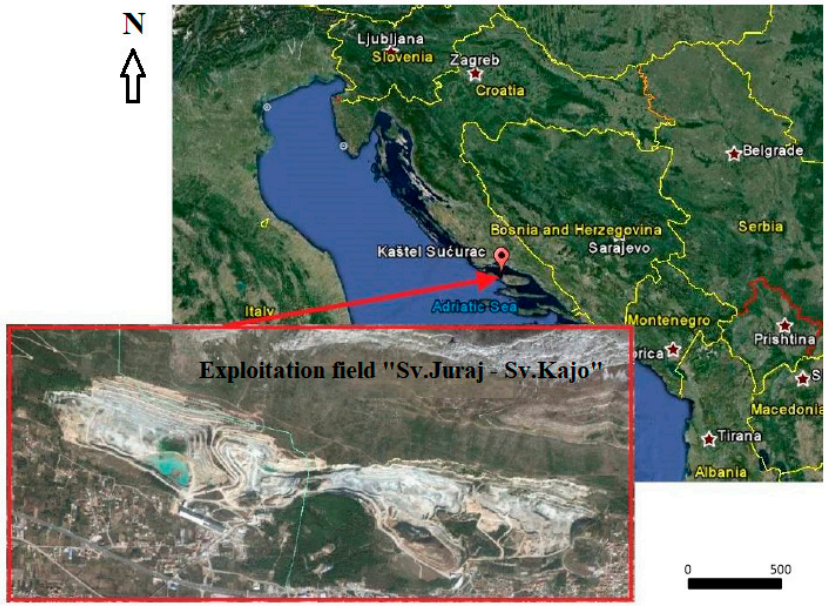

Figure 1. Geographic location of the exploited field "St. Juraj–St. Kajo" (after [19]).

The flysch is a dominant lithology, which is a descriptive term used to denote the facies of marine sedimentary rocks. The facies are characterized by high-powered sections of faunal-poor, thin-layered sediments with gradation stratification, represented mainly by marls, sandy and calcareous shales, and silts rhythmically interlacing with conglomerates, coarse-grained sandstones, and graywacke. A widespread pre-Orogenic sedimentary formation formed by a set of flysch facies deposited in various deflections as a result of the rapid erosion of nearby mountain structures uplifting during the period immediately preceding the main phase of orogeny, or during the erosion of the internal ridges created in the early phases of diastrophism. For example, the flysch layers of the late Cretaceous–Oligocene period along the borders of the Alps, which filled the marginal deflections before the tectonic covers advanced to the north prior to the main (Miocene) phase of Alpine orogeny. It is a term used freely to refer to any sediment having the most lithological and stratigraphic features of flysch, for example, almost any turbidites. Dalmatian flysch can reach at outcrops of up to 700 m thickness [10]. According to [7], in the Lutetian (Middle Eocene) period the depositional areas sunk, causing transgression and fast, variable and generally thick sedimentation of clastics (flysch) in deeper environments, supported by strong tectonics. The flysch [3] is divided into three stratigraphic zones: lower, middle, and upper. Furthermore, the two upper zones have been analysed, and the middle is divided into three lithological members: lower debrites, middle calcarenites, and upper marl [7,8,10,11]. The upper flysch included changes of marl and sandstone with alterations of the conglomerate. The flysch is also named "olistostrome" [11], where the upper flysch is divided into three members: lower, middle (sandstone), and upper (conglomerate), including "clips zone" with large, limy blocks with mud support (a kind of megabed). Based on petrology, clastics are described as the following lithological units [14] based on $CaCO_3$ content: nummulitic (micro) breccia (77–80% $CaCO_3$); calcarenite and calcsiltite (80–95% $CaCO_3$); marly limestone (77–80% $CaCO_3$); limy marl (75–77% $CaCO_3$); marl and clayey marl (65–74% $CaCO_3$); marl with redeposited nummulite (highly variable $CaCO_3$); and alternations of marl, sandstone, and limestone (55–70% $CaCO_3$). This lithological classification, with a correction of the percentage of $CaCO_3$ in nummulitic (micro) breccia, is used today. In the exploited field the strata direction is NW–SE with a dip towards the N–NE of around 30°–40°.

In the raw material deposits the following lithological units are proven (Figure 2): (1) marl/sandstone changes with conglomerate alterations; (2) limy (calcitic) marl; (3) calcsiltite (clayey limestone); (4) calcarenite; (5) nummulitic marl; and (6) debrites (Figure 3a–f) [20]. Here,

clayey marl (7) is also added, as lithofacies of the marginal parts of (1) and (5). The units (6) are divided into the western and eastern layer and all others into the northern and southern layer [20].

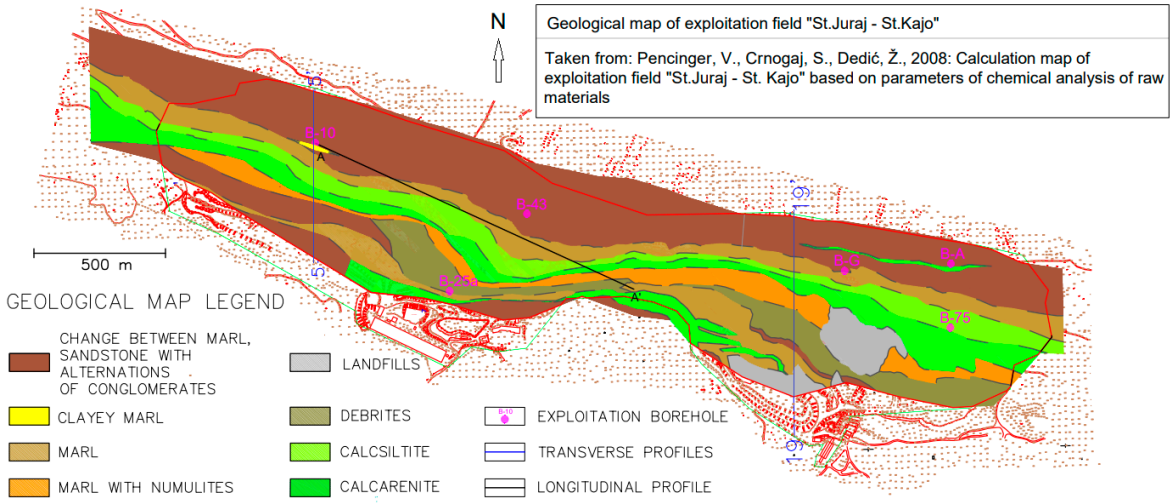

Figure 2. Geological map of the field of exploitation "St. Juraj–St. Kajo" (modified according to [20]).

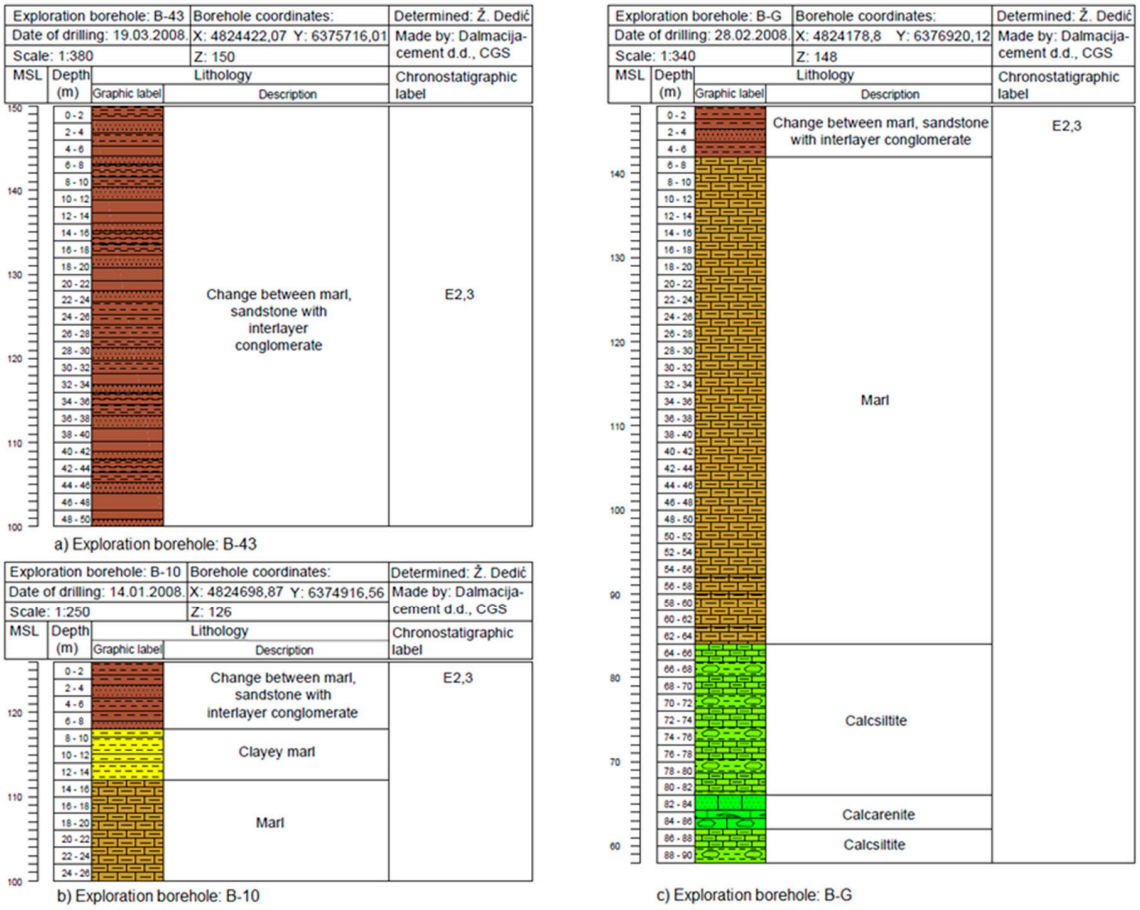

Figure 3. *Cont.*

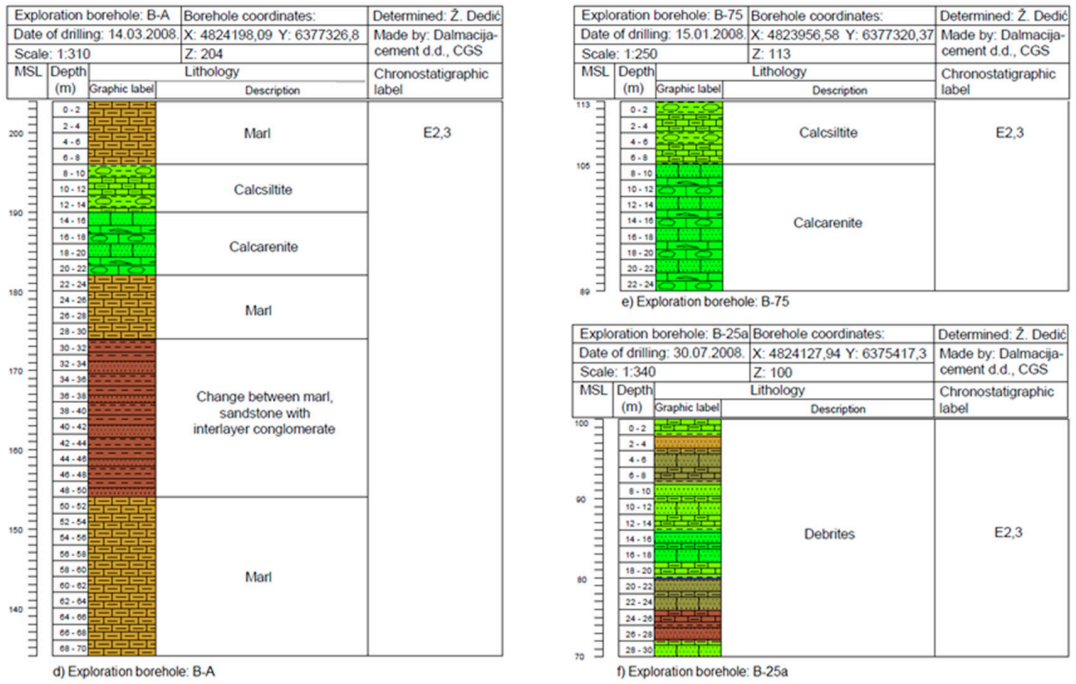

Figure 3. Geological sections: (**a**) exploration borehole B-45: lithological unit marls and sandstones with alterations of conglomerates; (**b**) exploration borehole B-10: lithological unit clayey marl; (**c**) exploration borehole B-G: lithological unit marl; (**d**) exploration borehole B-A: lithological unit calcsiltite; (**e**) exploration borehole B-75: lithological unit calcarenite; (**f**) exploration borehole B-25a: lithological unit debrites.

Unit 1—marl and sandstone with (sometimes thick) alterations of conglomerate are the lithological units covering the largest area. Marls significantly contribute to the upper part, and calcarenites can be found thinly bedded, from fine to coarse-grained. Sporadic detritus is coarse, with a sand component in marls, calcarenites, or think sandstones (5–60 cm). Generally, they are poorly sorted with some noncarbonate components (chert, other quartz, feldspar, pyrite, glauconite, coal) but rarely more than 30%. At the base of the northern layer calcitic (or sporadically clayey) marl can be found. In the southern layer, the top and bottom borders are not clearly recognizable. The data for statistical testing was collected from thirty-six exploration boreholes in the northern layer and seven boreholes in the southern layer.

Unit 2—clayey marl included a significant clay portion and is not extended over the entire field but forms thin interlayers. The data for statistical testing was collected from 18 exploration boreholes in the northern and 27 boreholes in the southern layers.

Unit 3—calcitic marl was found continuously throughout the entire field. It has an ideal portion of $CaCO_3$ (74–77.5%) for use as cement raw material. Locally, it can be replaced with clayey limestone. It is, due to tectonics and atmospheric influence, medium to highly weathered, often forming talus. The data for statistical testing was collected from 26 exploration boreholes in the northern and 14 boreholes in the southern layers.

Unit 4—calcsiltite is of a fine-grained texture with carbonate organic detritus. It was found in transitional facies between calcitic marl and calcarenite, extended in lenses over the entire field. It gradually changes into calcarenite at the base and in different facies at the top. The data for statistical testing were collected from 28 exploration boreholes in the northern and 24 boreholes in the southern layers.

Unit 5—calcarenite is a hard lithological unit, with a fine-grained texture of organic carbonate detritus. Rarely, quartz and glauconite pebbles were found, with parts consisting of foraminifera and corals. Calcarenite can be followed through the entire field. The data for statistical testing was collected from 18 exploration boreholes in the northern layer and 4 boreholes in the southern layer.

Unit 6—nummulite marls include elongated nests of nummulites (breccia) and other parts of foraminifera and reefs. The number of preserved nummulites has decreased, and the skeleton remains larger towards the top, gradually changing into calcarenite.

Unit 7—debrites are a chaotic unit with large clasts (olistolites), including shallow water limestones and deep-water, mud-supported sediments. Limestones are represented with Eocene foraminifera limestones (biomicrite), including glauconite, and limestones with chert. Additionally, Cretaceous limestone clasts with rudists and sparite with Orbitolinae and green algae can be found. Basinal deposits include thin calcarenite, marl (also in clasts and as clast support), and sandstone. This unit has a normal graduation with increasing mud support in the upper part. The data for statistical testing was collected from seven exploration boreholes in the western layer and five boreholes in the eastern layer.

2. Technological Characteristics of the Selected Lithological Units

All described lithological units in the field are raw materials of different quality. Their technological ranking is based on chemical compounds, and they are mixed in different ratios with the purpose of reaching the desired technological level, i.e., quality. There are four main oxides: CaO, SiO_2, Al_2O_3, and Fe_2O_3, used as ranking parameters of each unit. The weighting ratios of those oxides define three cement modules—lime saturation factor (LSF, Equation (1)), silicate module (SM, Equation (2)), and aluminate module (AM, Equation (3)).

The lime saturation factor is the ratio between effective (real) CaO content vs. CaO that can be bounded to other oxides (SiO_2, Al_2O_3, Fe_2O_3) during the process of burning and cooling of clinker [21]. The raw material with LSF = 90–98 is considered a good burning material. The LSF > 100 resulted in the rest of the CaO remaining as lime, and LSF < 90 allows for easier burning but leaves a coating in the rotary kiln.

$$\mathrm{LSF} = \left[\frac{\mathrm{CaO}}{2.8\mathrm{SiO_2} + 1.18\mathrm{Al_2O_3} + 0.65\mathrm{Fe_2O_3}}\right] * 100 \quad (1)$$

The silicate module is the ratio between SiO_2 vs. Al_2O_3 and Fe_2O_3 [22]. The values are 1.9–3.2. The SM $\leq$ 2 causes an increase in the liquid phase that supports burning, but also forms of thick coating in the kiln. The SM $\geq$ 3 results in the decreasing of liquid and consequently the burning of clinker is weaker, leaving a thin coating in the kiln.

$$\mathrm{SM} = \frac{\mathrm{SiO_2}}{\mathrm{Al_2O_3} + \mathrm{Fe_2O_3}} \quad (2)$$

The aluminate module is the ratio of Al_2O_3 and Fe_2O_3 which defines liquid content in clinker, i.e., the temperature of liquid forming and viscosity [22]. The value is 1–2.5. The larger AM causes a larger melt viscosity and the harder creation of the clinker minerals. Additionally, if the liquid is created too early, the process will start at an untimely point, creating the rings in the kiln.

$$\mathrm{AM} = \frac{\mathrm{Al_2O_3}}{\mathrm{Fe_2O_3}} \quad (3)$$

At the beginning of exploitation, in the 1950s, the field was technologically divided into three raw material types, based on the LSF values, as follows: (1) high, (2) normal, and (3) low. A further subzone can be extracted using the SM value. Moreover, the single unit can belong to multiple zones, such as nummulite marl and debrites. The ranking values are:

1. High raw material (LSF > 110):
   - calcarenite: LSF > 250, SM = 2–3
   - calcsiltite: LSF = 110–250, SM = 2.5–3.5
   - nummulite marl: LSF = 110–250, SM = 2–3.5
   - debrites: LSF > 110, SM = 2.5–3.5.

2. Normal raw material (LSF = 90–110):
   - calcite marl: LSF = 90–110, SM = 2.4–2.8
   - nummulite marl: LSF = 90–110, SM = 2 – 3.5
   - debrites: LSF = 90–110, SM = 2.5–3.5.
3. Low raw material (LSF < 90):
   - marl/sandstone with conglomerate alterations: LSF = 60–80, SM = 3–8
   - nummulite marl: LSF = 80–90, SM = 2–3.5
   - clayey marl: LSF = 60–80, SM < 3
   - debrites: LSF < 90, SM = 2.5–3.5.

3. Materials and Methods

Geological sections in exploration wells are divided into 2 m intervals, where samples were taken for chemical, lithological, and chronostratigraphic analyses. Lithologies were previously defined in [20], now updated with clayey marl facies (LSF < 90 and SM < 3). Of the top and bottom of the layer, thicknesses of units, as well as coordinates, are given in Table 1. and Figure 4. Two transversal (5–5′ and 19–19′) and one longitudinal (A–A′) section are constructed (Figures 5 and 6). The previous solutions [22] are updated at the locations of exploration boreholes, reaching a more precise determination of the (inter)layers.

Table 1. Input data for the thickness calculations of the units.

Layer	Lithological Unit	Top layer (m)	Botom Layer (m)	Layer Thickness (m)	Data Number (−)
North layer	Change between marl, sandstone with alternation of conglomerates	159	148	11	36
	Clayey marl	135	125	10	18
	Marl	130	115	15	26
	Calcsiltite	120	110	10	28
	Calcarenite	105	89	16	18
Western layer	Debrites	102	78	22	7
South layer	Change between marl, sandstone with alternations of conglomerates	96	93	3	7
	Clayey marl	101	94	7	27
	Marl	101	95	6	14
	Calcsiltite	105	97	8	24
	Calcarenite	103	100	3	4
Eastern layer	Debrites	119	89	25	5
					Σ = 214

Furthermore, statistical analyses were carried out using the chemical data (XRF analyses) of nine compounds (CaO, SiO_2, Al_2O_3, Fe_2O_3, MgO, SO_3, Na_2O, K_2O, $CaCO_3$ (%)) and three cement modules (LSF, SM, AM), collected in six lithological units (1, 2, 3, 4, 5, 7). Th normality of data was tested using Kolmogorov–Smirnov (K–S) and Shapiro–Wilk (S–W) tests. The total number of data was n = 214, with a single set including 4 to 36 points. The α value was 0.05. The sets with n < 30 were tested with K–S, and those with n > 30 using the S–W test.

Statistical tests were applied as more formal procedures compared with graphical tools (histogram, QQ plots) which can be used for normality tests [23]. Different formal tests can be chosen regarding strength and critical values [24], but all of them can be applied for most geological variables, which mostly complied with the central limit theorem (stating that a large number of independently sampled data inclined to normal/Gaussian distribution, e.g., [25]). Here, the two formal tests selected were K–S and W–S, as previously mentioned [26,27].

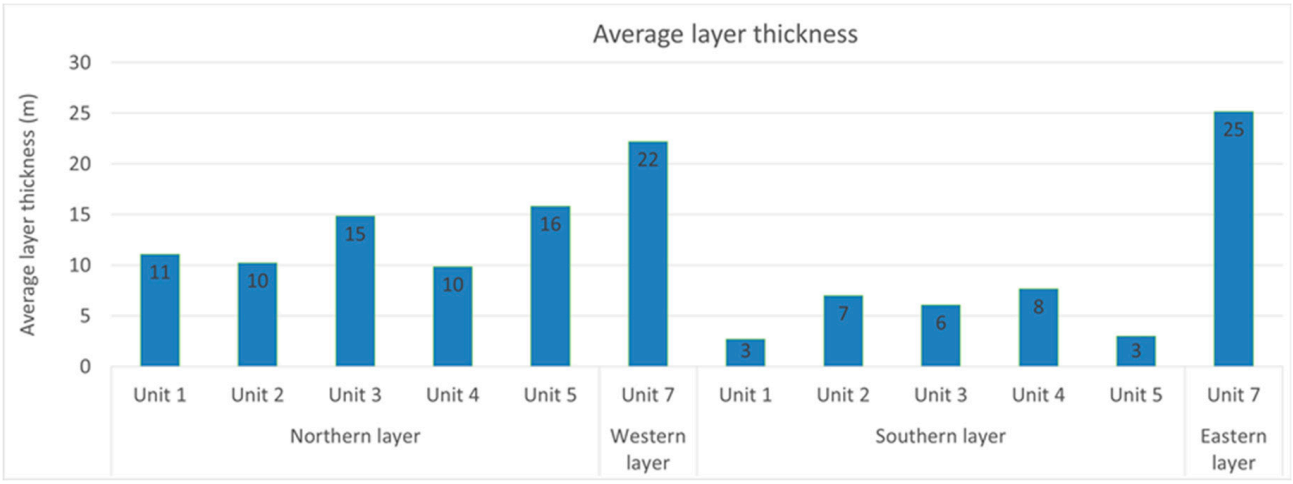

Figure 4. Average thickness of lithological units in the analysed layers.

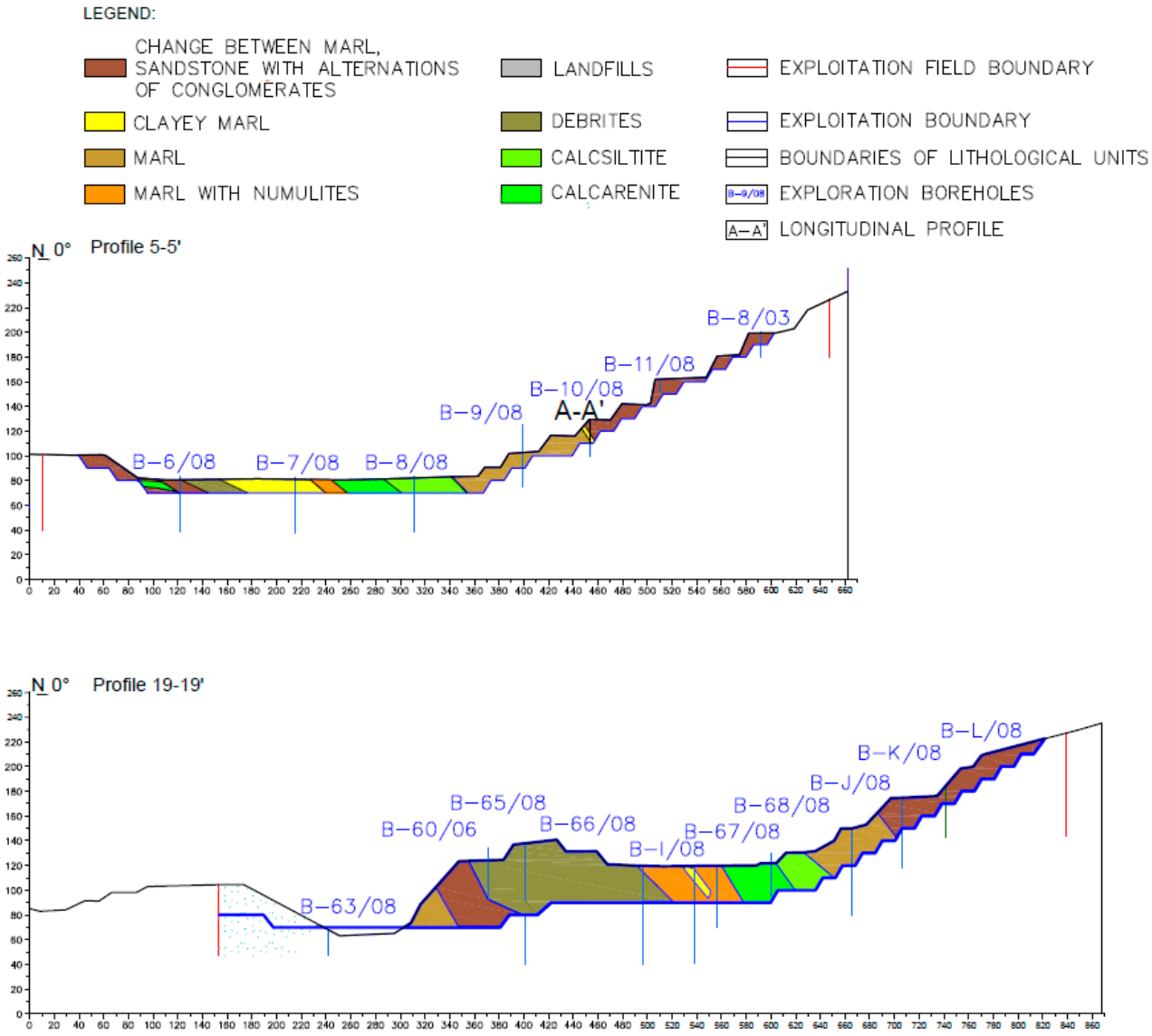

Figure 5. Transversal geological cross-sections 5–5′ and 19–19′.

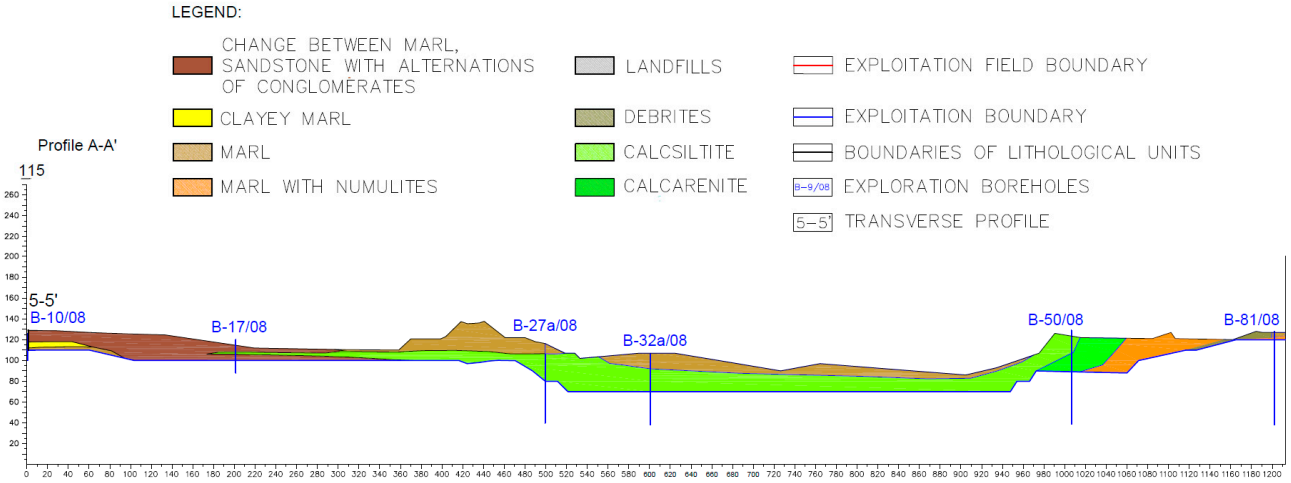

Figure 6. Longitudinal geological cross-section A–A'.

3.1. Kolmogorov-Smirnov Test

Nonparametric formal tests are not dependent on distribution, i.e., mean and variance are not known (e.g., [25]). K–S is one of the most used nonparametric formal normality tests for the distribution of one or two samples. It compares empirical distribution function (EDF) with theoretical cumulative distribution function (CDF) using the calculation of distance given in Equation (4) [28]:

$$Dn = \frac{sup}{x}|F_n(x) - F(x)| \tag{4}$$

where:

n—size of sampled set
supx—supremum of distances
Fn(x)—empirical cumulative distribution function (EDF)
F(x)—theoretical cumulative distribution function (CDF)

3.2. Shapiro–Wilk Test

Shapiro-Wilk test (S–W test) uses a null-hypothesis, assuming that normal distribution exists, with *p*-value as the highest possibility that such data do not exist, but null-hypothesis can be accepted (e.g., [29]). Statistical values (W) are between 0 (test failed) and 1 (data are normally distributed—e.g., [23]), and calculation is carried out using Equation (5) [30]:

$$W = \frac{\left(\sum_{i=1}^{n} a_i x_{(i)}\right)^2}{\sum_{i=1}^{n}(x_i - \overline{x})^2} \tag{5}$$

where:

W—test statistics
ai—constant
x(i)—statistics of i-th order
$\overline{x}$ *= (x1 +· · · + xn)/n—mean value of samples*
n—number of samples

Interpolation was performed in three lithological units as follows: (1) marl/sandstone with alterations of conglomerate—northern layer, (5) calcarenite—northern layer, and (7) debrites—western layer. In all units, collected values of CaO (%), SiO_2 (%) and cement module LSF (−) were found. The mapping was carried out using two methods: ordinary kriging (OK) and inverse distance weighting (IDW). The selection was based on normality

tests results. If data had normal distribution the mapping was carried out by kriging, and if they did not have normality, inverse distance weighting was applied. The problem of small datasets ($n < 15$), like in debrites, was nonreliable testing. Consequently, in such a case IDW was (again) applied. In units (1) and (5) all maps (CaO (%), SiO_2 (%), and LSF (−)) were created using OK, and in the unit (7) using IDW (Table 2).

Table 2. Input data, formality tests results, and interpolation methods for units (1), (5), and (7).

Lithological Unit	Statistic		Mapping					
			CaO (%)		SiO_2 (%)		LSF (−)	
	Data Number (*n*)	Normality Test	Test Outcome	Interpolation Method	Test Outcome	Interpolation Method	Test Outcome	Interpolation Method
Change between marl, sandstone with alternations of conglomerates—norther layer	36	SW	Pass	OK	Pass	OK	Pass	OK
Calcarenite—northern layer	18	KS	Pass	OK	Pass	OK	Pass	OK
Debrites—western layer	7	KS	Pass	IDW	Pass	IDW	Fail	IDW

3.3. Kriging

Kriging is interpolation based on the calculation of the weighting coefficients added to known values. Such values depend on only distances among unknown values and locations of known values. The kriging matrix calculation minimizes estimation variance, using experimental and theoretical variogram models of data (e.g., [31]). Variograms ($2y$) as graphical tools for the determination of spatial dependence are calculated using Equation (6) [32]:

$$2y(h) = \frac{1}{n}\sum_{i=1}^{n}[z(x_i) - z(x_i + h)]^2 \quad (6)$$

where:

2y(h)—variogram value
n—number of data pairs at distance "h"
$z(x_i)$—value at location "x_i"
$z(x_i + h)$—value at location distant for "h" from location "x_i"

The experimental variogram is most often approximated with spherical, exponential, Gaussian, or linear theoretical models. The variogram models are also distinguished regarding the existence of the nugget effect or not [33].

3.4. Inverse Distance Weighting

Inverse distance weighting [34] is a mathematically simpler method where an unknown value is estimated using known values in a searching radius, weighting them according to their distance. The general form is given in Equation (7) [35]:

$$z_{iu} = \frac{\sum_{i=1}^{n}\frac{z_i}{d_i^p}}{\sum_{i=1}^{n}\frac{1}{d_i^p}} \quad (7)$$

where:

z_{iu}—estimated value
d_i—distance to the "i-th" location
z_i—known value at the "i-th" location
p—power exponent for distance

The influence of each known value is inversely proportional to its distance from a location with an unknown value. The result is largely influenced by the value "p" but, usually, it is set at 2 [32].

4. Results

The geological sections showed six lithological units: Unit 1—marl and sandstone with (sometimes thick) alterations; Unit 2—clayey marl; Unit 3—calcitic marl; Unit 4—calcsiltite; Unit 5—calcarenite, and Unit 6—debrites. The average thickness is calculated for all of them (Figure 4).

The spatial locations of cross-sections are given in Figure 2. and the details of the cross-sections in Figure 5 (transversal 5–5′ and 19–19′) and Figure 6 (longitudinal A–A′). Transversal revealed the positional of the units in the northern and southern layers, including thin intercalations and longitudinal thinning along the strike.

In total, 144 formal normality tests were performed, 132 K–S and 12 S–W tests, of these 71% of tests passed; results given in Table 3 (green passed, red failed). The lowest pass level is calculated for the oxides SO_3 (58%) and K_2O (33%) and the cement modules SM (42%) and AM (50%). The highest pass is attributed to the oxides Al_2O_3, Fe_2O_3, and MgO (92%). If lithological units are considered, the lowest pass can be observed in the marl from the northern layer (25%) and the highest in debrites, from both the western and eastern layers (92%).

Table 3. Passable levels for the normality tests for oxides and cement modules vs. lithological units.

Lithological Units		Chemical Characteristics									Cement Modules			Pass Rate
		SiO_2	Al_2O_3	Fe_2O_3	CaO	MgO	SO_3	Na_2O	K_2O	$CaCO_3$	LSF	SM	AM	
Change between marl, sandstone with alternations of conglomerates—northern layer	SW test $n = 36$; $\alpha = 0.05$	+	+	+	+	+	−	+	−	+	+	−	−	67%
	p	0.2848	0.3077	0.0827	0.1800	0.0577	0.0436	0.0776	0.0180	0.1803	0.1783	0.0000	0.0007	
Change between marl, sandstone with alternations of conglomerates—southern layer	KS test $n = 8$; $\alpha = 0.05$	+	+	+	−	−	+	+	+	−	−	−	+	58%
	p	0.0652	0.0784	0.0963	0.0194	0.0183	0.3973	0.3802	0.0791	0.0198	0.0257	0.0162	0.7911	
Clayey marl—northern layer	KS test $n = 18$; $\alpha = 0.05$	+	+	+	+	+	+	+	−	+	+	−	+	83%
	p	0.4312	0.6364	0.8022	0.8059	0.0849	0.1441	0.8625	0.0000	0.8008	0.5899	0.0321	0.1137	
Clayey marl—southern layer	KS test $n = 27$; $\alpha = 0.05$	+	+	+	+	+	+	+	−	+	+	−	−	75%
	p	0.0881	0.0723	0.2051	0.4998	0.2029	0.2989	0.1453	0.0001	0.4935	0.4322	0.0000	0.0002	
Marl—northern layer	KS test $n = 26$; $\alpha = 0.05$	−	+	−	−	+	−	+	−	−	−	−	−	25%
	p	0.0004	0.0632	0.0354	0.0022	0.1178	0.0002	0.3153	0.0000	0.0021	0.0060	0.0276	0.0000	
Marl—southern layer	KS test $n = 14$; $\alpha = 0.05$	+	+	+	+	+	+	−	−	+	+	+	+	83%
	p	0.2608	0.1904	0.0677	0.3273	0.1078	0.5297	0.0491	0.0000	0.3299	0.5425	0.1851	0.1065	
Calcsiltite—northern layer	KS test $n = 28$; $\alpha = 0.05$	+	+	+	+	+	−	−	−	+	+	+	−	67%
	p	0.7297	0.6069	0.4000	0.7610	0.4963	0.0000	0.0015	0.0002	0.7595	0.7079	0.1044	0.0003	
Calcsiltite—southern layer	KS test $n = 24$; $\alpha = 0.05$	−	−	+	+	+	−	+	−	+	−	−	−	42%
	p	0.0170	0.0021	0.7666	0.1105	0.2280	0.0105	0.6101	0.0029	0.1128	0.0044	0.0000	0.0343	
Calcarenite—northern layer	KS test $n = 18$; $\alpha = 0.05$	+	+	+	+	+	+	−	+	+	+	−	−	75%
	p	0.1573	0.8429	0.2380	0.8252	0.3341	0.0550	0.0192	0.0736	0.8188	0.4630	0.0243	0.0002	
Calcarenite—southern layer	KS test $n = 4$; $\alpha = 0.05$	+	+	+	+	+	−	+	+	+	+	+	+	92%
	p	0.2607	0.7948	0.2787	0.2413	0.1976	0.0107	0.6603	0.9273	0.2400	0.2216	0.3421	0.3788	
Debrites—western layer	KS test $n = 7$; $\alpha = 0.05$	+	+	+	+	+	+	+	+	+	−	+	+	92%
	p	0.6479	0.1508	0.2862	0.5895	0.1094	0.6915	0.3960	0.2639	0.6201	0.0280	0.2487	0.2891	
Debrites—eastern layer	KS test $n = 5$; $\alpha = 0.05$	+	+	+	+	+	+	+	−	+	+	+	+	92%
	p	0.6430	0.7450	0.3448	0.0871	0.8986	0.3906	0.5844	0.0494	0.0879	0.7707	0.6347	0.3404	
	Passrate	83%	92%	92%	83%	92%	58%	75%	33%	83%	67%	42%	50%	71%

For available data, the nine maps were interpolated. Unit (1), in the northern layer, was interpolated by OK, for variables CaO (%), SiO_2 (%), and LSF (−). The experimental variogram was calculated using the nugget C = 0, sills CaO = 3, SiO_2 = 5, LSF = 145, range a = 240 m, total calculation distance h = 1033 m, number of classes 15, and tolerance 45°. The approximation was carried out using the exponential model (Figure 7). Variograms defined searching ellipsoid with axes 240 × 50 m, directions −15° and 105°, and anisotropy factor 4.8. The maps of CaO (%), SiO_2 (%), and LSF for the unit (1) in the northern layer are shown in Figures 8–10.

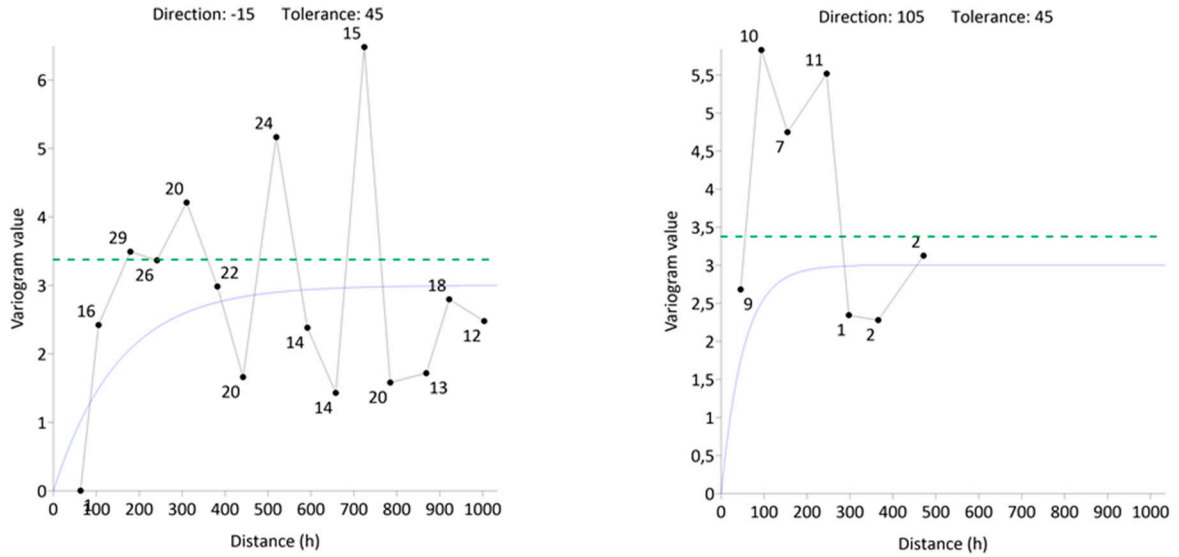

Figure 7. Variograms for the unit (1), northern layer.

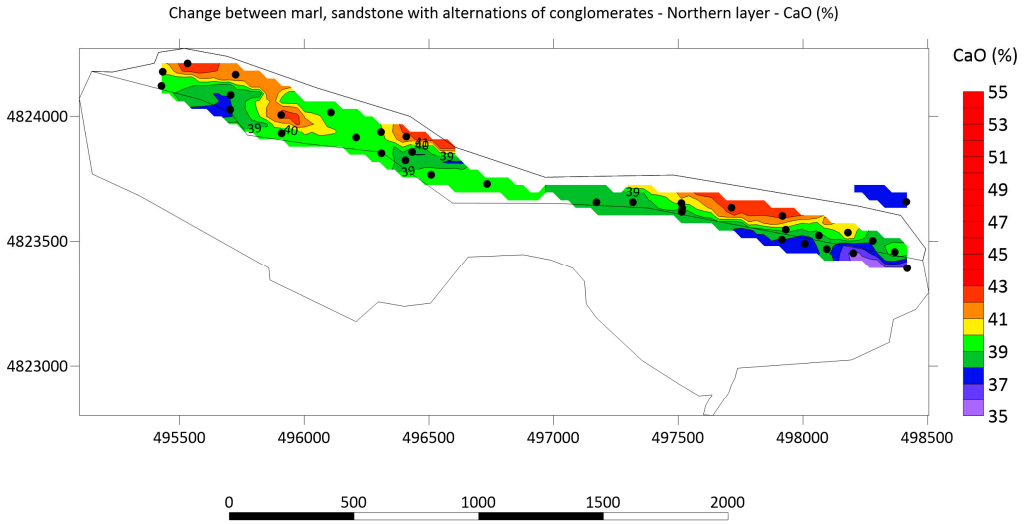

Figure 8. Map of CaO (%) in unit (1), northern layer (boreholes are black dots).

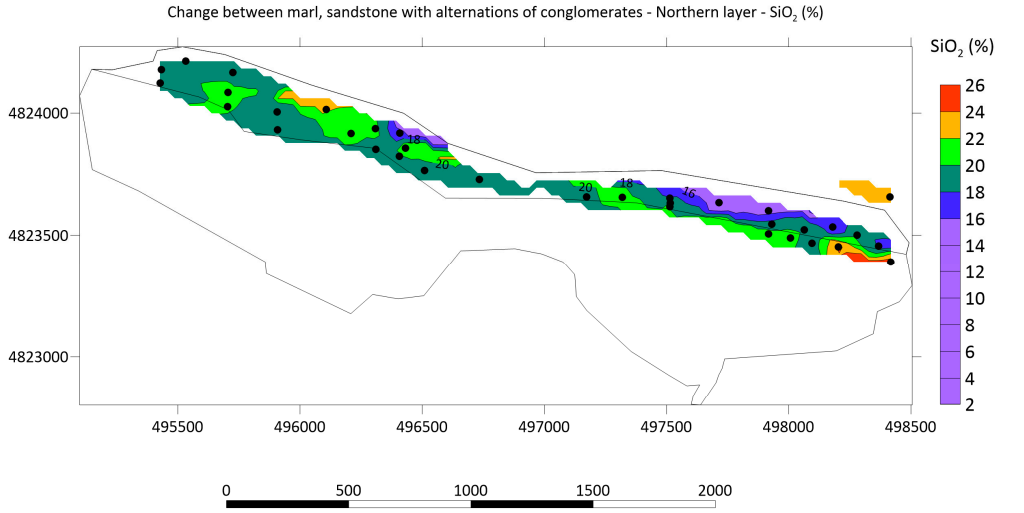

Figure 9. Map of SiO_2 (%) in unit (1), northern layer (boreholes are black dots).

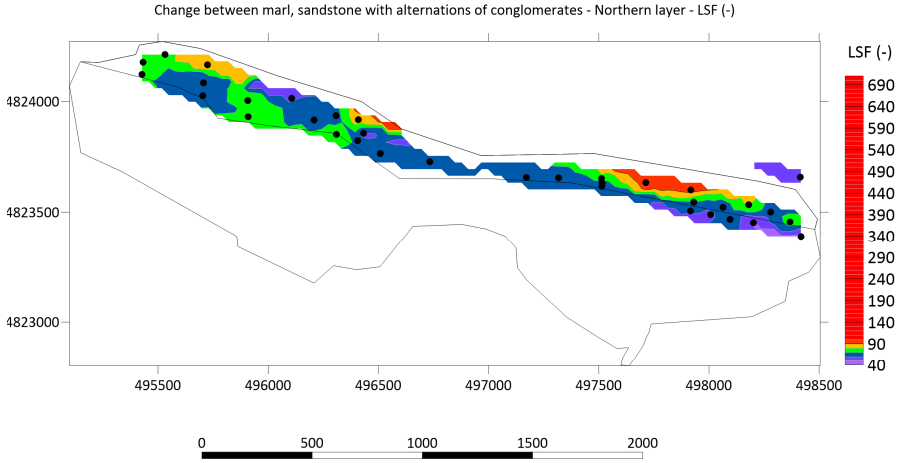

Figure 10. Map of LSF (−) in unit (1), northern layer (boreholes are black dots).

The three maps in unit (5), in the northern layer, showed values of CaO (%), SiO_2 (%), and LSF (−). All were interpolated by ordinary kriging, using the nugget Co = 0, sill C(CaO) = 1, C(SiO_2) = 1, C(LSF) = 15,000, range a = 320 m, total calculation distance h = 1033 m, number of classes 17, and tolerance 45°. The experimental variogram was approximated with the exponential model (Figure 11). The searching ellipsoid had axes of 320 × 50 m with strikes −15° and 105° and an anisotropy factor 6.4. The maps of CaO (%), SiO_2 (%), and LSF (−) are shown in Figures 12–14.

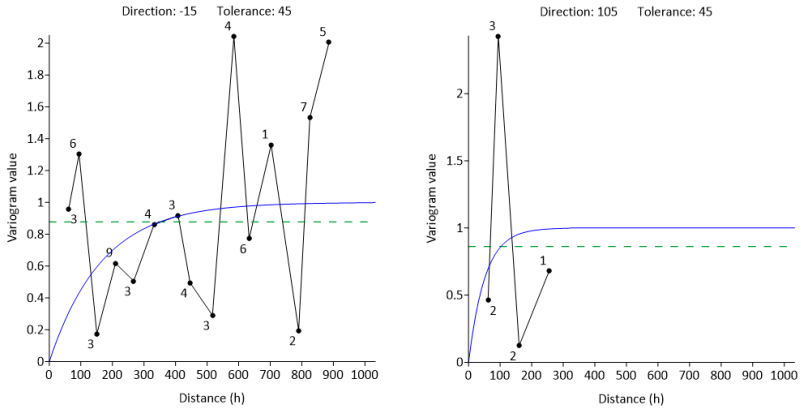

Figure 11. Variograms for unit (5), northern layer.

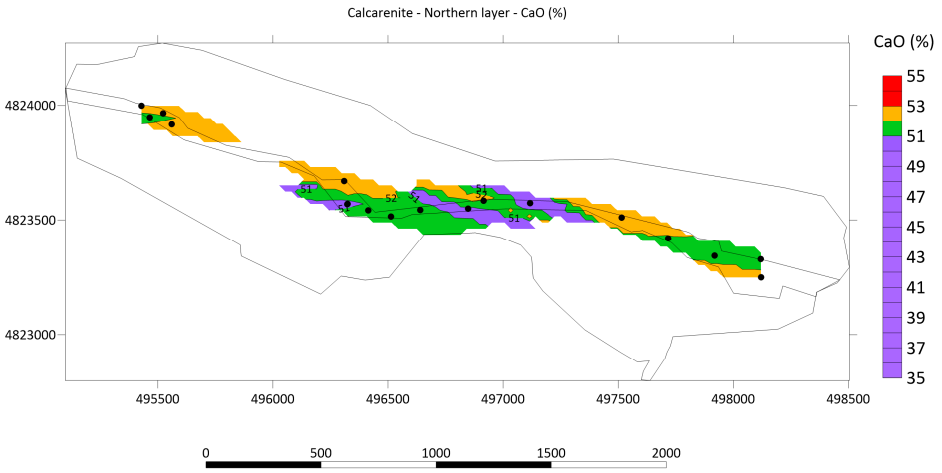

Figure 12. Map of CaO (%) in unit (5), northern layer (boreholes are black dots).

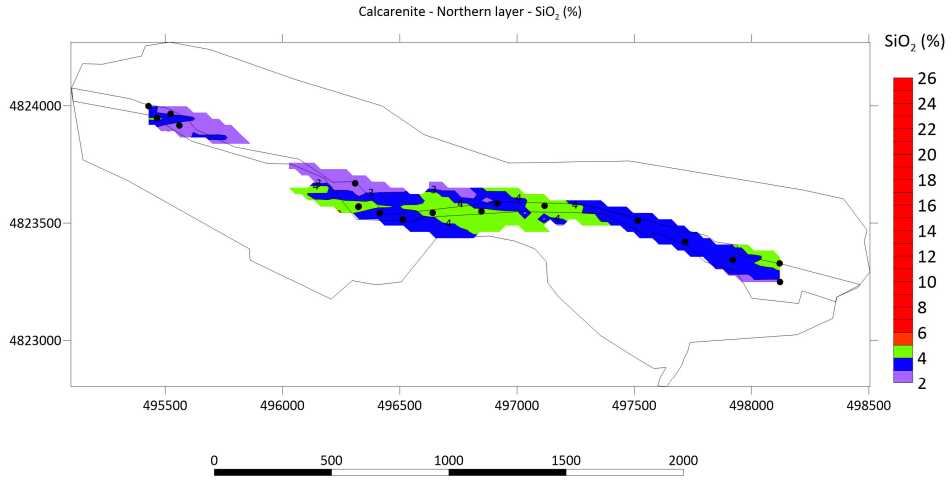

Figure 13. Map of SiO_2 (%) in unit (5), northern layer (boreholes are black dots).

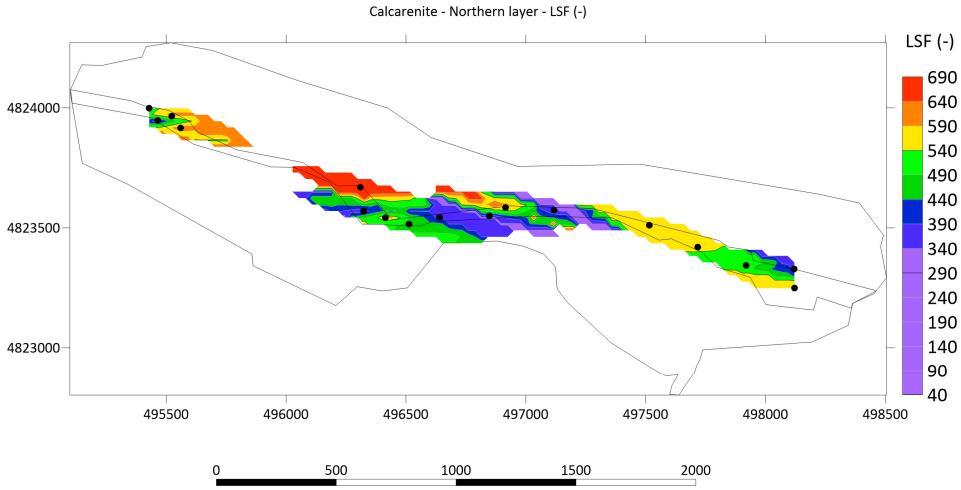

Figure 14. Map of LSF (−) in unit (5), northern layer (boreholes are black dots).

The last three maps were interpolated for unit (7), in the western layer. Interpolation for CaO (%), SiO_2 (%) and LSF (−) was carried out using IDW. Power exponent was 2, searching circle 335 m, and anisotropy = 1 (no anisotropy). The maps are given in Figures 15–17.

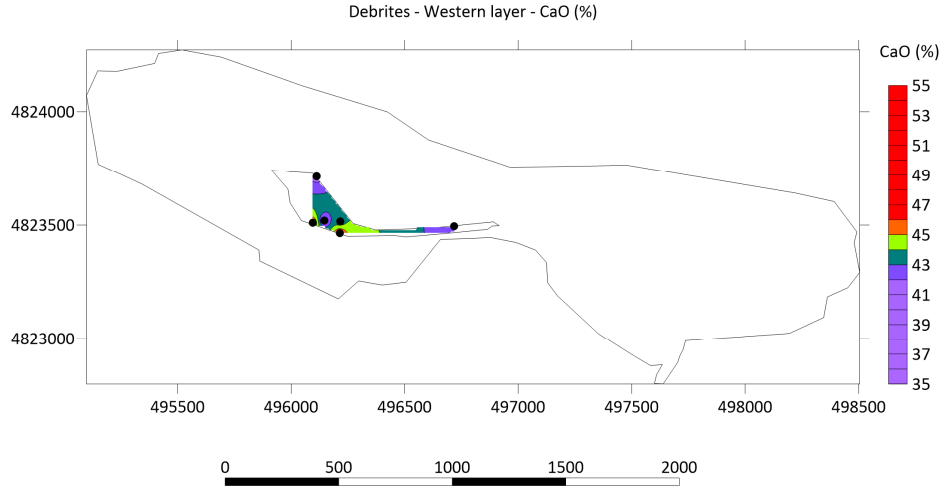

Figure 15. Map of CaO (%) in unit (7), western layer (boreholes are black dots).

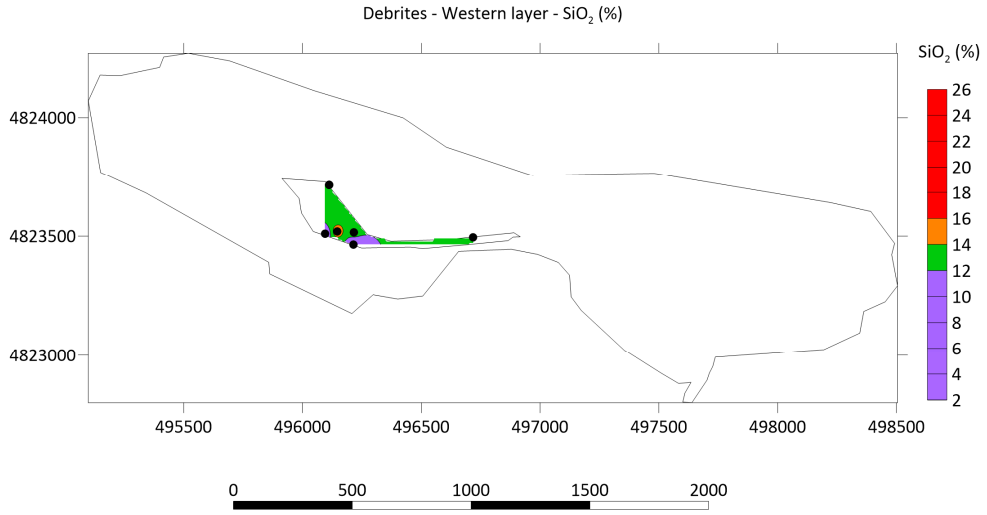

Figure 16. Map of SiO_2 (%) in unit (7), western layer (boreholes are black dots).

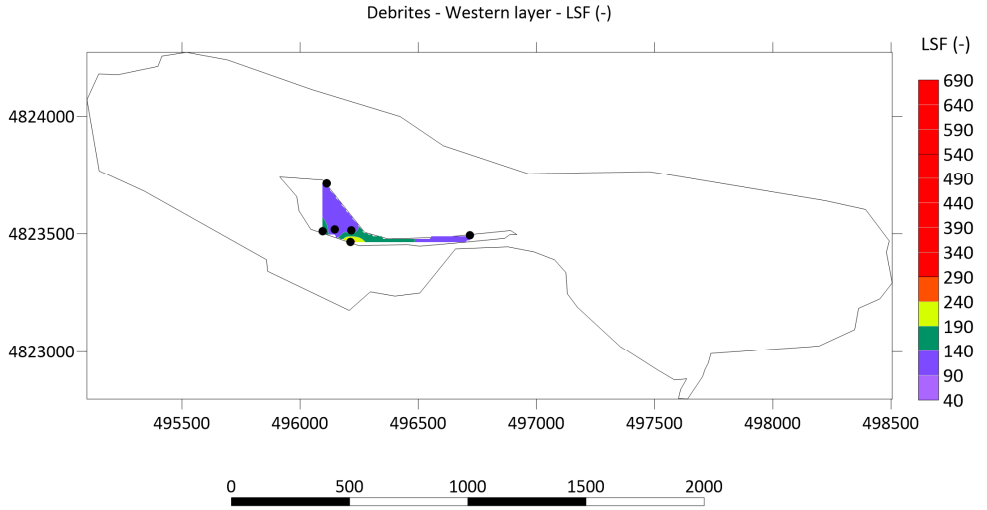

Figure 17. Map of LSF (−) in unit (7), western layer (boreholes are black dots).

5. Conclusions

Statistical analyses of oxides and cement modules of the flysch raw material were performed. The samples were taken in the field of exploitation "St. Juraj–St. Kajo", near Split, southern Croatia, where raw material is exploited for cement production. Three components were analysed, namely the oxides SiO_2 and CaO (%) and the cement module "lime saturation factor" (LSF) (−). Out of the seven lithological units, three of them were selected for detailed mapping as follows: unit (1), marl/sandstone with alterations of conglomerate in the northern layer; unit (5), calcarenite in the northern layer; and unit (7), debrites in the western layer.

Thickness analysis showed that beds in the northern layer are about two times thicker than in the southern one, but also included more clayey intercalations. Furthermore, the 144 datasets were analysed with formal normality tests, namely the Kolmogorov–Smirnov and Shapiro–Wilk tests. In total, 71% of datasets (including 7–35 data) showed normal (Gaussian) distribution.

All three lithological units (1, 5, 7) were interpolated with three characteristic maps of oxides CaO and SiO_2 and the cement module LSF. Unit 1 (with a layer width of 200–300 m and 36 datapoints) showed that CaO and LSF values slightly decreased toward the south, but values of SiO_2 varied by 18–20%. Unit 5 (with a layer width of 50–150 m and 18 datapoints) showed that CaO concentrations were slight, but SiO_2 was highly variable

throughout the unit. However, the LSF values were gradual, but very variable, reaching even 300 m, which is crucial information for quality control. Analysis showed unit 7 to be the most irregular (with a width of 30–200 m and 7 datapoints), with the largest variations of all three variables on small scales.

The results are the most extensive statistical and mapping analysis of an expoited raw cement material field in the last decade. It was possible to estimate chemical compounds and cement modules in any part of the field for the three analysed units. This is especially important because the final raw material is obtained by mixing different raw materials exploited from different units. It is the first time this amount of data from exploration boreholes has been collected, analysed with formal normality tests, and eventually interpolated with one of two chosen methods. This has made it possible to fulfil current quality control conditions during the production of clinker and cement, but also to support further reserve calculations.

Author Contributions: Conceptualization, N.B. and T.M.; Formal analysis, N.B. and T.M.; Investigation, N.B.; Software, T.M. and N.B.; Supervision, T.M.; Validation, N.B.; Visualization, N.B.; Writing—original draft, N.B.; Writing—review and editing, N.B. and T.M. All authors have read and agreed to the published version of the manuscript.

Funding: This research received no external funding.

Acknowledgments: The geological sections were created using licensed AutoCAD software. Statistical tests were performed using a calculator available on the statskingdom page. Interpolations were carried out using the licensed Surfer 23 program. This research was partially carried out in the project "Mathematical researching in geology VI" (led by T. Malvić) and for doctoral study exploration (N. Bralić).

Conflicts of Interest: The authors declare no conflict of interest.

References

1. Kerner, F.v. Geologische Spezijalkarte Der Oester. Ung. Mon., Zone 31, Kol XV, Blatt Sinj Und Spalato, 1:75,000—k.k. Geologische Reichsanstalt, 1914, Wien. Available online: https://www.hgi-cgs.hr/arhivske-karte-austrougarske (accessed on 22 March 2022).
2. Kerner, F.v. *Die Geologischen Verhältnisse Der Poljen von Blaca Und Konjsko Bei Spalato*; Separatdruck; Geologisch-Paläontologisches Anstalt der Universität Basel: Basel, Switzerland, 1902.
3. Kerner, F.v. Gliederung der Spalatiner Flyschformation, Verh. geol. R. A., 1903, Wien. Available online: https://www.zobodat.at/pdf/VerhGeolBundesanstalt_1903_0085-0087.pdf (accessed on 30 March 2022).
4. Kerner, F.v. Zur geologie von Spalato (Entgegung an prof Carlo de Stefani und A. Martelli). Verh. geol. R. A., 1905, 16, Wien. Available online: https://www.zobodat.at/pdf/VerhGeolBundesanstalt_1905_0127-0165.pdf (accessed on 30 March 2022).
5. Schubert, R. Geologische Fuhrer Durch Damatien, Sammlung geol. Fiihrer, 1909, 14, Berlin. Available online: https://opac.geologie.ac.at/ais312/dokumente/VH1909_234_A.pdf (accessed on 30 March 2022).
6. Schubert, R. *Geologija Dalmacije*; Matica Dalmatinska: Zadar, Croatia, 1909.
7. Marinčić, S. Paleogene breccias of the wider Mosor area. *Geološki Vjesn.* **1970**, *23*, 113–119. (In Croatian)
8. Lukšić, B. *Research for the Cement Industry in the Wider Area of Split—Quarry "Partizan"*; 232, Zagreb; Fund p. while. Cemex Croatia d.d.: Kaštel Sućurac, Crotia, 1976. (In Croatian)
9. Marinčić, S.; Korolija, B.; Mamužić, P.; Magaš, N.; Majcen, Ž.; Brkić, M.; Benček, Đ. *Interpreter of the Basic Geological Map M 1: 100,000 for Omiš, K 33-22*; Map: Beograd, Sebia, 1977. (In Croatian)
10. Marinčić, S. Eocene flysch of the Adriatic belt. *Geol. Vjesn.* **1981**, *34*, 27–38. (In Croatian)
11. Marjanac, T. Sedimentation of Kerner's "middle flysch zone" (Paleogene, Split area). *Geol. Vjesn.* **1987**, *40*, 177–194. (In Croatian)
12. Marjanac, T. Reflected sediment gravity flows and their deposits in flysch of Middle Dalmatia, Yugoslavia. *Sedimentology* **1990**, *37*, 921–929. [CrossRef]
13. Tomašić, I. Limitation of contours of mineral raw materials in the deposit space with regard to quality. *Rud.-Geol.-Naft. Zb.* **1990**, *2*, 177–181. (In Croatian with English Abstract).
14. Matijaca, M.; Vujec, S. Statistical interpretation of raw materials for the cement industry in Split. *Rud.-Geol.-Naft. Zb.* **1990**, *2*, 75–81. (In Croatian with English Abstract).
15. Marjanac, T. Deposition of Megabeds (Megaturbidites) and Sea-Level Change in a Proximal Part of Eocene-Miocene Flysch of Central Dalmatia (Croatia). *Geol. Boulder* **1996**, *24*, 543–546. [CrossRef]
16. Miščević, P.; Roje-Bonacci, T. Weathering process in eocene flysch in region of Split (Croatia). *Rud.-Geol.-Naft. Zb.* **2001**, *13*, 47–55.
17. Pollak, D.; Buljan, R.; Toševski, A. Engineering-Geological and Geotechnical Properties of Flysch Formations in Kaštela Region. *Građevinar* **2010**, *62*, 8.

18. Žižić, D.; Bartulović, H. Dietzsch cement kilns and their significance for the industrial architecture of Dalmatia. Prost. *Znan. Časopis Arhit. Urban.* **2015**, *23*, 42–55. (In Croatian)
19. Parlov, J.; Hrženjak, P.; Bralić, N.; Terzić, J. Comparison of the Hydraulic Conductivities Calculated from Pumping Tests and Discontinuities in the Middle Eocene Flysch Basin, Exploitation Field Sv. Juraj-Sv. Kajo, Croatia. In Proceedings of the 42nd IAH Congress, Rome, Italy, 13–18 September 2015.
20. Pencinger, V.; Ožanić, M.; Crnogaj, S.; Dedić, Ž.; Jurić, A. *Study on the Reserves of Mineral Raw Materials for the Production of Cement in the Exploitation Field "St. Juraj—Sv. Kajo "-Restoration*; Croatian Geological Survey: Zagreb, Croatia, 2009. (In Croatian)
21. Kruk, B.; Dedić, Ž. *Study on the Reserves of Mineral Raw Materials for the Production of Cement in the Exploitation Field "St. Juraj—Sv. Kajo "-Restoration*; Croatian Geological Survey: Zagreb, Croatia, 2013. (In Croatian)
22. Duda, W.H. *Cement-Data-Book: International Process Engineering in the Cement Industry*; Bauverlag: Gütersloh, Germany, 1985.
23. Nornadiah, M.R.; Yap, B.W. Power comparisons of Shapiro-Wilk, Kolmogorov-Smirnov, Lilliefors and Anderson-Darling tests. *J. Stat. Modeling Anal.* **2011**, *2*, 21–33.
24. Yazici, B.; Yolacan, S. A comparison of various tests of normality. *J. Stat. Comput. Simul.* **2007**, *77*, 175–183. [CrossRef]
25. Malvić, T.; Medunić, G. Statistics in Geology. In *Textbooks of the University of Zagreb*; Faculty of Mining, Geology and Petroleum Engineering and Faculty of Science, University of Zagreb: Zagreb, Croatia, 2015; 88p.
26. Kolmogorov-Smirnov Test Calculator: Normality Calculator, Q-Q Plot. Available online: https://www.statskingdom.com/kolmogorov-smirnov-test-calculator.html (accessed on 24 March 2022).
27. Shapiro-Wilk Test Calculator: Normality Calculator, Q-Q Plot. Available online: https://www.statskingdom.com/shapiro-wilk-test-calculator.html (accessed on 24 March 2022).
28. Dimitrova, D.S.; Kaishev, V.K.; Tan, S. Computing the Kolmogorov-Smirnov Distribution When the Underlying CDF Is Purely Discrete, Mixed, or Continuous. *J. Stat. Softw.* **2020**, *95*, 1–42. [CrossRef]
29. Šapina, M.; Vekić, M. New lithostratigraphic units of the Croatian coast and their provisions in the "R" programming language. *Rud.-Geol.-Naft. Zb.* **2015**, *30*, 13–24, (In Croatian with English Abstract). [CrossRef]
30. Shapiro, S.S.; Wilk, M.B. An analysis of variance test for normality (complete samples). *Biometrika* **1965**, *52*, 591–611. [CrossRef]
31. Malvić, T.; Cvetković, M.; Balić, D. *Geomathematic Dictionary*; Croatian Geological Society: Zagreb, Croatia, 2008; 74p. (In Croatian)
32. Mesić Kiš, I. Comparison of ordinary and universal kriging interpolation techniques on a depth variable (a case of linear spatial trend), case study of the Šandrovac field. *Rud.-Geol.-Naft. Zb.* **2016**, *31*, 2. [CrossRef]
33. Malvić, T. Application of Statistics in the Analysis of Geological Data. In *Textbooks of the University of Zagreb*; INA-Oil Industry d.d.: Zagreb, Croatia, 2008; 103p.
34. Malvić, T.; Ivšinović, J.; Velić, J.; Sremac, J.; Barudžija, U. Application of the Modified Shepard's Method (MSM): A Case Study with the Interpolation of Neogene Reservoir Variables in Northern Croatia. *Stats* **2020**, *3*, 68–83. [CrossRef]
35. Malvić, T.; Ivšinović, J.; Velić, J.; Rajić, R. Interpolation of Small Datasets in the Sandstone Hydrocarbon Reservoirs, Case Study of the Sava Depression, Croatia. *Geoscience* **2019**, *9*, 201. [CrossRef]